CONSTRAINED INTERPOLATION AND SHAPE PRESERVING APPROXIMATION BY SPACE CURVES

KONG VOON PANG

UNIVERSITI SAINS MALAYSIA

2006

CONSTRAINED INTERPOLATION AND SHAPE PRESERVING APPROXIMATION BY SPACE CURVES

by

KONG VOON PANG

Thesis submitted in fulfilment of the requirements for the degree of Doctor of Philosophy

February 2006

ACKNOWLEDGEMENTS

I would like to take this opportunity to acknowledge the contributions of numerous people to this thesis, beginning with my supervisor, Prof. ONG BOON HUA from the School of Mathematical Sciences, Universiti Sains Malaysia. I am very grateful and appreciate her invaluable support, guidance, supervision in my research and the preparation of this thesis.

My sincere appreciation to the Universiti Sains Malaysia especially the Dean of the School of Mathematical Sciences and the Dean of Institute of Graduate Studies for allowing me to pursue my higher degree here and granting me the scholarship under the scheme Biasiswa Khas sponsored by the Ministry of Science, Technology and Innovation. I would like to acknowledge the financial support of the Fundamental Research Grant of Malaysia and thank the School of Mathematical Sciences for the utilization of facilities.

I also wish to thank my lover, parents and family members as well as friends for their support and encouragement. Lastly, I would like to dedicate this thesis to the mighty God.

TABLE OF CONTENTS

LIST OF TABLES

LIST OF FIGURES

LIST OF APPENDICES

LIST OF PUBLICATIONS

INTERPOLASI BERKEKANGAN DAN PENGHAMPIRAN MENGEKAL BENTUK DENGAN LENGKUNG RUANG

ABSTRAK

Dua jenis masalah rekabentuk lengkung telah dipertimbangkan. Terlebih dahulu kami mempertimbangkan interpolasi satu set titik data ruang yang bertertib dengan satu lengkung licin tertakluk kepada satu set satah kekangan yang berbentuk terhingga atau tak terhingga di mana garis cebis demi cebis yang menyambung titik data secara berturutan tidak bersilang dengan satah kekangan. Satu kaedah interpolasi setempat diterbitkan supaya lengkung Bézier kubik nisbah cebis demi cebis yang dijana adalah selanjar secara G^2 dan tidak bersilang dengan sebarang satah kekangan yang diberi. Sifat-sifat geometri Bézier kubik nisbah dicirikan dan dieksploitasikan dalam penerbitan syarat-syarat untuk mengelakkan persilangan di antara lengkung interpolasi dengan satah kekangan.

Seterusnya, penghampiran lengkung mengekal bentuk dipertimbangkan untuk memadankan satu lengkung pada satu set titik data ruang bertertib. Satu skema penghampiran dipersembahkan bagi penjanaan satu lengkung splin kubik penghampiran C^2 yang mengekal bentuk. Di samping itu, satu pendekatan geometri juga dipersembahkan untuk mengekstrak titik-titik knot daripada satu set nilai parameter yang pelbagai. Kami mentakrifkan poligon yang menyambung titik data yang bersepadan dengan jujukan knot terpilih sebagai bentuk asas set data. Syarat cukup dalam bentuk linear untuk kriteria pengekalan bentuk tentang sifat kecembungan, lengkok balas, kekolinearan dan kesesatahan dicadangkan untuk memastikan lengkung penghampiran memimik bentuk set data. Splin penghampiran diperoleh dengan menyelesaikan satu masalah kuasa dua terkecil tertakluk kepada syarat-syarat linear pengekalan bentuk.

ABSTRACT

Two types of curve designing problem have been considered. We first consider the interpolation of a given set of ordered spatial data points by a smooth curve in the presence of a set of finite or infinite constraint planes, where the polyline joining consecutive data points does not intersect with the constraint planes. A local method is presented for the construction of a G^2 constrained piecewise rational cubic interpolant which does not cross the given constraint planes. The geometrical properties of the Bézier rational cubics are characterized and exploited in the derivation of conditions for the interpolant to avoid crossing the constraint planes.

Next, the shape preserving curve approximation is considered for fitting a curve to an ordered set of spatial data points. A scheme is presented for the construction of a C^2 shape preserving cubic spline approximant. A geometric approach is also presented for extracting the knots from a large set of parameter values. We define the polyline connecting the associated data points on the selected knot sequence as the shape of the data. Linear sufficient conditions for shape preserving criteria on convexity, inflections, collinearity and coplanarity are proposed to ensure the approximant mimics the shape of the data. The approximating spline curve is obtained by solving a least square problem subject to linear conditions of shape preservation.

CHAPTER 1
INTRODUCTION

Computer aided geometric design (CAGD) is concerned with the approximation and representation of the curves and surfaces that arise when these objects have to be processed by a computer. Designing curves plays an important role in the manufacturing of products such as aircrafts and ship hulls, in the modelling of paths of robots and particles, in abstract and physical processes in economics, social and physical sciences, in the description of geological and medical phenomena, and in numerous other situations.

In this thesis, two types of curve designing problem have been considered. We first discuss the interpolation of a given set of spatial data points by a smooth curve in the presence of a set of finite or infinite constraint planes, where the polyline joining consecutive data points does not intersect the constraint planes. Next the shape preserving curve approximation is considered for fitting a curve to a large set of ordered spatial data points.

1.1 Constrained Interpolation

The stylist and designer usually demand that interpolation and approximation methods accurately represent physical reality. They require the behaviour of the resulting curve to conform to the ‘shape’ of the data. For example, when a non-negative physical quantity is visualized by an interpolating curve, the latter should not admit negative values. Investigation on non-negativity preserving interpolation has been pursued to address this problem and much has been done in this respect, such as (Schmidt & Hess, 1988), (Wever, 1988), (Opfer & Oberle, 1988), (Dougherty et al., 1989) and (Lahtinen, 1993).

A number of attempts have also been made to consider the more general problem, namely range restricted interpolation, where the interpolant could be parametric or non-parametric, and as the name suggests, the interpolant is constrained to lie within a specified region. Arbitrary straight lines and quadratic curves instead of just the horizontal straight lines have been used as the boundaries of the admissible region, see (Goodman et al., 1991), (Ong & Unsworth, 1992), (Butt & Brodlie, 1993), (Zhang & Cheng, 2001) and (Meek et al., 2003). All the interpolating curves considered in the references cited above are planar curves.

In (Goodman et al., 1991) interpolation to planar data points that lie on one side of one or more straight lines has been considered. The line considered is an infinite line. The necessary and sufficient conditions on the Bézier control points and the weights in order to ensure that the interpolant does not cross a given constraint line are derived. A local scheme was described for generating a G^2 (i.e. the unit tangent vector and curvature vary continuously along the curve) parametric rational cubic spline which lies on the same side of these constraint lines as the data points. This scheme is based on the piecewise rational cubic scheme described in (Goodman, 1988). Meek et al. (2003), extend the scheme described in (Goodman et al., 1991) to generate for a given set of ordered planar points lying on one side of a polyline, a planar G^2 interpolating curve which also lies on the same side of the polyline. This allows the polyline as a more general constraint where all the data points need not lie on one side of the infinite line through each of its edges.

In addition, the two schemes above generate curves which are shape preserving in the sense that they have the minimal number of inflections consistent with the data. These rational schemes reproduce circles and are invariant under a rotation or a change in scale.

We are not aware of any schemes on the problem of range restricted curve interpolation in space. We consider the problem of constrained interpolation by parametric space curves with planes as constraints. This extends the works of (Goodman et al., 1991) and (Meek et al. 2003) from the two dimensional to the three dimensional setting. This type of constrained interpolation could be useful in problems like designing a smooth space curve that must fit within a specified region or generating a smooth robot's path in space that avoids obstacles (corners or polyhedral objects) in the navigation of mobile robots (McKerrow, 1991).

Given a finite sequence of space data points and constraint planes where the polyline connecting consecutive data points does not intersect with these constraint planes. We explore and characterize the corresponding geometrical structures of the Bézier rational cubics to derive a method which generates constrained G^2 interpolating space curves that avoid intersection with any given constraint planes. The necessary and sufficient conditions described in (Goodman et al., 1991) and (Meek et al. 2003) are generalized for the rational cubic in space so that it does not cross a given constraint plane.

The constrained interpolation in space is presented in four chapters. We characterize the geometrical properties of the parametric rational cubic Bézier space curves in Chapter 2. The rational curve of the form $\boldsymbol{R}(t,\alpha,\beta)$, $t \in [0,1]$ in (2.2) with positive weights α , $\beta > 0$ is considered, where the corresponding control polygon ***ABCD*** is not planar. Three geometrical structures, namely the β -surface, the α -surface and the *t*-triangle are obtained from $\boldsymbol{R}(t,\alpha,\beta)$ by respectively holding the parameter β , α and *t* fixed while allowing the other two to vary. Each family of these structures fills the interior of the tetrahedron with the control points of $\boldsymbol{R}(t,\alpha,\beta)$ as its vertices. The "nested" and "layered" properties of these structures are exploited in the construction of the constrained interpolating curve in avoiding the intersection with the given constraint planes. In Chapter 3, the necessary and sufficient conditions for a rational cubic Bézier to touch a plane are derived. The construction of the constrained interpolating curve together with an algorithm is given in Chapter 4. Test results of the suggested scheme and conclusion are given in Chapter 5.

1.2 Shape Preserving Approximation

In practical fields such as medicine, engineering, physics and computer graphics the amount of data obtained through experimental and statistical surveys is usually very large. The use of an interpolation scheme for the construction of spline curves from the given data consisting of a relatively large number of points will yield a huge number of curve segments. Besides, in most applications the points are subject to measurement errors. We can hope that with the curve approximation, these errors will more or less be smoothed out and the resulting curve may look smooth enough.

Shape preserving approximation of planar and space data has played an important role in curve fitting over a large amount of data. As mentioned at the beginning of previous section, it is often required that the approximating curve should reveal certain properties of the curve underlying the data. Another reason why the shape preserving conditions were imposed is that they may prevent undesirable inflection or oscillations of the curve. The contributions to the case of shape preserving approximation by spline functions include the articles (Elfving & Anderson, 1988), (Schmidt & Scholz, 1990), (Elliott, 1993), (Dierckx, 1996) and (Kvasor, 2000). In (Jüttler, 1997) and (Morandi et al., 2000), parametric planar spline curves are obtained, and it seems only (Costantini & Pelosi, 2001) described the construction of shape preserving curves which approximate an ordered set of spatial data.

Since a large amount of data points are approximated by means of a spline approximation scheme, so the selection of a suitable and reliable small set of knots becomes an indispensable step. The determination of the number and the positions of the knots are not nearly as simple where non-linear formulation is involved via the approximation criterion. Lyche and Mørken (1987, 1988) use the approach, namely knot removal, to obtain these parameters by reducing an initial large set of knots involved in an approximation problem. In (Tuohy et al., 1997), (Morandi et al., 2000) and (Costantini & Pelosi, 2001), a knot sequence is extracted from the assigned parameter values using geometric information inherited in the data. We will also select a knot sequence through a geometric approach using the inherent discrete properties of the data points. In general, more knots should be placed in those regions where the data change rapidly or have complex shapes.

In (Dierckx, 1996), sufficient conditions for a spline function to be convex are discussed. These conditions are first developed by the author in 1980 for the cubic spline approximation. The approximant is then obtained by minimizing the approximation errors between the given points and the approximating curve subject to linear convexity conditions. Jüttler (1997) generalizes the algorithm of Dierckx to the case of planar parametric curves. Using a reference curve, the author generates linear sufficient convexity conditions. The approximating curve is then obtained as the minimum of a quadratic programming problem with linear convexity conditions. In (Morandi et al., 2000) the definition of the shape is automatically determined by a geometric approach and the parametric spline curve is constructed via an optimisation problem with non-linear convexity conditions. We note that all the approximating curves considered above are B-spline curves.

Costantini and Pelosi (2001) have extended the planar results to the spatial case. Non-linear shape preserving constraints are imposed and the tension properties of the variable degree polynomial spline are used to construct the shape preserving curve approximating the data. If the least square approximant (obtained by minimizing a non-constrained least square problem) fails to satisfy the shape preserving constraints, the degree of the splines are increased until the approximant satisfies the constraints.

To our knowledge, no work has appeared on shape preserving approximation of spatial data with linear constraints. Since a linearly constrained optimisation problem can be solved faster and in a numerically more stable fashion than one with non-linear constraints, we propose a new method for the construction of an approximating curve in space subject to linear constraints for shape preservation.

Given a sequence of spatial data points, we develop a geometric approach for extracting a proper subset of knots from the large set of parameter values. Subsequently we define the polyline connecting the associated data points of the selected knots as the shape of the data. Based on this polyline, denoted as l_U, we are able to generate linear sufficient constraints for the shape preservation of the approximating spline curve. The shape constraints involved convexity, inflection, collinearity and coplanarity, while the constraints on the sign of torsion are not included since it is not clear how to linearize such constraints. Cubic B-spline is recommended to construct the C^2 approximating curve which gives a good compromise between the quality of fit and efficiency in computation time and memory requirements. It also enables the shape preserving criteria to be formulated in a very simple way. The above selected knots constitute the knot sequence of the B-splines. The de Boor points of the approximant are determined as the optimal solution of a quadratic programming problem subject to the above linear shape constraints.

The outline of the shape preserving approximation in space is as follows. In Chapter 6 we present a strategy to extract knots from the assigned parameter values, using geometric information such as the discrete tangent, the discrete binormal and the sign of discrete torsion determined from the data points. In that chapter we also describe the construction of the polyline l_U, used for defining the shape of the data. The description of the shape preserving criteria and some useful properties of B-spline are recalled in Chapter 7. The linearly constrained least square problem is also stated. Chapter 8 describes the generation of the linear sufficient conditions for the approximant to mimic the shape of the polyline l_U. Finally, the algorithms, some numerical results to illustrate our shape preserving curve approximation scheme and the conclusion are given in Chapter 9.

CHAPTER 2
PARAMETRIC RATIONAL CUBIC BÉZIER SPACE CURVE

2.0 Introduction

Rational Bézier spline curves have been widely implemented in computer aided geometric design specifically for conic sections which cannot be represented exactly in the usual (non-rational) Bézier form. Consider the parametric rational cubic Bézier curve in space

$$\boldsymbol{R}(t, w_0, w_1, w_2, w_3) = \frac{w_0(1-t)^3\boldsymbol{A} + w_1 3t(1-t)^2\boldsymbol{B} + w_2 3t^2(1-t)\boldsymbol{C} + w_3 t^3\boldsymbol{D}}{w_0(1-t)^3 + w_1 3t(1-t)^2 + w_2 3t^2(1-t) + w_3 t^3}, \; 0 \le t \le 1, \quad (2.1)$$

with the weights $w_i > 0$, $0 \le i \le 3$, and the control points $\boldsymbol{A}$, $\boldsymbol{B}$, $\boldsymbol{C}$, $\boldsymbol{D} \in \nabla^3$. If all the weights equal one, we obtain the non-rational Bézier curve, where in this case the denominator is identically equal to one. In general, two weights w_i, w_j can always be chosen to be 1 since this can always be achieved by an appropriate transformation. Thus, we can take $w_1 = w_2 = 1$ and rewrite (2.1) as

$$\boldsymbol{R}(t, \alpha, \beta) = \frac{\alpha(1-t)^3\boldsymbol{A} + 3t(1-t)^2\boldsymbol{B} + 3t^2(1-t)\boldsymbol{C} + \beta t^3\boldsymbol{D}}{\alpha(1-t)^3 + 3t(1-t)^2 + 3t^2(1-t) + \beta t^3}, \quad 0 \le t \le 1, \qquad (2.2)$$

with the weights α, $\beta > 0$, and $\boldsymbol{A}$, $\boldsymbol{B}$, $\boldsymbol{C}$, $\boldsymbol{D} \in \nabla^3$.

Rational Bézier curve with positive weights enjoy all the properties that their non-rational counterparts possess. With α, β as fixed and abbreviating $\boldsymbol{R}(t, \alpha, \beta)$ as $\boldsymbol{R}(t)$, we have the following formulas

$$\boldsymbol{R}(0) = \boldsymbol{A}, \qquad \boldsymbol{R}(1) = \boldsymbol{D},$$

$$\boldsymbol{R}'(0) = \frac{3(\boldsymbol{B}-\boldsymbol{A})}{\alpha}, \qquad \boldsymbol{R}'(1) = \frac{3(\boldsymbol{D}-\boldsymbol{C})}{\beta},$$

$$\kappa(0) = \frac{2\alpha\|(\boldsymbol{B}-\boldsymbol{A})\times(\boldsymbol{C}-\boldsymbol{B})\|}{3\|\boldsymbol{B}-\boldsymbol{A}\|^3}, \qquad \kappa(1) = \frac{2\beta\|(\boldsymbol{C}-\boldsymbol{B})\times(\boldsymbol{D}-\boldsymbol{C})\|}{3\|\boldsymbol{D}-\boldsymbol{C}\|^3}, \qquad (2.3)$$

where “ $'$ “ denotes the differential operator $\frac{d}{dt}$, $\kappa(0)$ and $\kappa(1)$ are the curvatures of $\boldsymbol{R}(t)$ at $t=0$ and $t=1$, and $\|\cdot\|$ denotes the magnitude of a vector. The rational curve $\boldsymbol{R}(t)$, $t \in [0, 1]$ is affine invariant, lies in the convex hull of its control points, i.e. the tetrahedron ***ABCD***, and has the variation diminishing property as stated below.

Proposition 2.1

The number of times a given plane crosses the rational cubic curve given by (2.2) is no more than the number of crossings that the polyline ***ABCD*** has with this plane.

The proof for this proposition can be easily adapted from the one given in (Goodman, 1989) for the parametric planar Bézier curve with any straight line.

As the case of the parametric Bézier rational cubic in ∇^2 has been explored in (Meek et al., 2003), let us assume that ***A***, ***B***, ***C***, ***D*** are not coplanar for otherwise the rational cubic would be a planar curve. In the following sections, we shall describe some simple and significant geometric properties of $\boldsymbol{R}(t, \alpha, \beta)$ which can be obtained by considering its first partial derivatives. Three geometrical structures, named as the β-surface, α-surface and the *t*-triangle are derived from $\boldsymbol{R}(t, \alpha, \beta)$ by respectively holding one of β, α and *t* fixed while allowing the other two to vary. Each family of these structures fill the interior of the tetrahedron ***ABCD***.

2.1 Cone-Shaped β-Surface and α-Surface

We shall first describe the limiting properties of the rational cubic $\boldsymbol{R}(t, \alpha, \beta)$ together with appropriate notations, and later the effect on the curve by varying one of its weights α or β. Observe that for $t \in (0, 1)$ and $\beta > 0$,

$$\lim_{\alpha \to 0} \boldsymbol{R}(t,\ \alpha,\ \beta) = \frac{3(1-t)^2\boldsymbol{B} + 3t(1-t)\boldsymbol{C} + \beta t^2\boldsymbol{D}}{3(1-t)^2 + 3t(1-t) + \beta t^2} \tag{2.4}$$

and

$$\lim_{\alpha \to \infty} \boldsymbol{R}(t,\ \alpha,\ \beta) = \boldsymbol{A}.$$

We shall denote the former limit as $\boldsymbol{R}(t,\ 0,\ \beta)$ while the latter as $\boldsymbol{R}(t,\ \infty,\ \beta)$. $\boldsymbol{R}(t,\ 0,\ \beta)$ is a rational quadratic in *t* with control polygon ***BCD***. So it lies in the triangle ***BCD*** of tetrahedron ***ABCD***. Similarly, for $t \in (0,\ 1)$ and $\alpha > 0$,

$$\lim_{\beta \to 0} \boldsymbol{R}(t,\ \alpha,\ \beta) = \frac{\alpha(1-t)^2\boldsymbol{A} + 3t(1-t)\boldsymbol{B} + 3t^2\boldsymbol{C}}{\alpha(1-t)^2 + 3t(1-t) + 3t^2}$$

and

$$\lim_{\beta \to \infty} \boldsymbol{R}(t,\ \alpha,\ \beta) = \boldsymbol{D},$$

and these two limits are denoted by $\boldsymbol{R}(t,\ \alpha,\ 0)$ and $\boldsymbol{R}(t,\ \alpha,\ \infty)$ respectively. Clearly, $\boldsymbol{R}(t,\ \alpha,\ 0)$ is a rational quadratic in *t* which lies in the triangle ***ABC***.

As reported in (Meek et al., 2003) for parametric planar cases, we have the first partial derivatives of $\boldsymbol{R}(t,\ \alpha,\ \beta)$ with respect to α and β as

$$\frac{\partial \boldsymbol{R}}{\partial \alpha}(t, \alpha, \beta) = \frac{(1-t)^3}{W(t, \alpha, \beta)^2}[3t(1-t)^2 + 3t^2(1-t) + \beta t^3][\boldsymbol{A} - \boldsymbol{R}(t, 0, \beta)], \tag{2.5}$$

$$\frac{\partial \boldsymbol{R}}{\partial \beta}(t, \alpha, \beta) = \frac{t^3}{W(t, \alpha, \beta)^2}[\alpha(1-t)^3 + 3t(1-t)^2 + 3t^2(1-t)][\boldsymbol{D} - \boldsymbol{R}(t, \alpha, 0)], \tag{2.6}$$

where $W(t, \alpha, \beta) = \alpha(1-t)^3 + 3t(1-t)^2 + 3t^2(1-t) + \beta t^3$. The consequences of the behaviour of these partial derivatives will be discussed in more detail in the subsections below.

2.1.1 β-Surface

As a direct consequence of (2.5), for any fixed $t_0 \in (0,\ 1)$ and $\beta_0 > 0$, as α increases from 0 to ∞, $\boldsymbol{R}(t_0,\ \alpha,\ \beta_0)$ moves along a straight line from the point

$\boldsymbol{R}(t_0,\ 0,\ \beta_0)$ in the triangle ***BCD*** towards ***A***. This geometric property gives rise to a cone-shaped constant β surface which we shall refer to as the β_0-surface, see Fig. 2.1(a). This surface consists of open line segments indexed by $t \in (0,\ 1)$ where each of the corresponding open line segments connects $\boldsymbol{R}(t,\ 0,\ \beta_0)$ to ***A***.

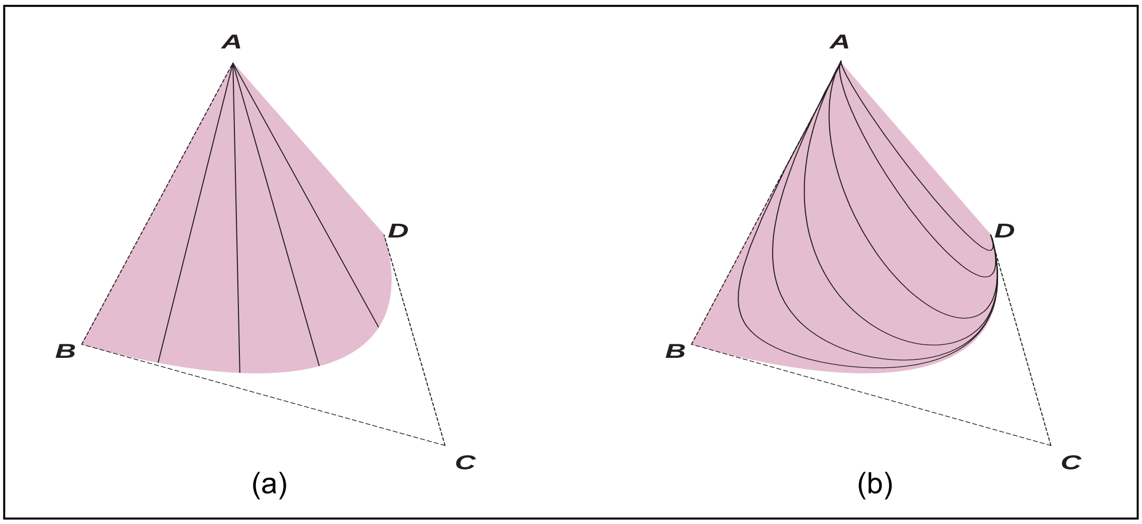

Fig. 2.1(a) β_0-surface, $\boldsymbol{R}(t,\ \alpha,\ \beta_0)$, $t \in (0,\ 1)$, $0 < \alpha < \infty$, for a fixed $\beta_0 > 0$, with some locus lines at $t = 0.2,\ 0.4,\ 0.6,\ 0.8$.

(b) Nested curves $\boldsymbol{R}(t,\ \alpha,\ \beta_0)$, $t \in (0,\ 1)$, for a fixed $\beta_0 > 0$ and $\alpha = 0.05$, 0.25, 1, 5, 50, 500, which lie on β_0-surface.

Furthermore, the β_0-surface also represents the family of rational cubic curves indexed by α, $\{\boldsymbol{R}(t,\ \alpha,\ \beta_0),\ t \in (0,\ 1):\ 0 < \alpha < \infty\}$, as illustrated in Fig. 2.1(b). For each fixed $\alpha > 0$, the corresponding rational cubic curve connects ***A*** to ***D***. Another consequence of the above geometric property is that this family of curves is nested, i.e. each rational cubic curve of the family does not intersect any other curve in the family.

The family of rational quadratics in (2.4) $\{\boldsymbol{R}(t,\ 0,\ \beta),\ t \in (0,\ 1):\ 0 < \beta < \infty\}$ actually coincides with the interior of triangle ***BCD***. Denoting by simple notations, we have

$$\boldsymbol{R}(t,\ 0,\ 0) = \lim_{\beta \to 0} \boldsymbol{R}(t,\ 0,\ \beta) = (1-t)\boldsymbol{B} + t\boldsymbol{C}$$

and

$$\boldsymbol{R}(t,\ 0,\ \infty) = \lim_{\beta\to\infty} \boldsymbol{R}(t,\ 0,\ \beta) = \boldsymbol{D}.$$

The first partial derivative of $\boldsymbol{R}(t,\ 0,\ \beta)$ with respect to β is

$$\frac{\partial \boldsymbol{R}}{\partial \beta}(t,\ 0,\ \beta) = \frac{3t^2(1-t)}{V(t,\ \beta)^2}[\boldsymbol{D} - [(1-t)\boldsymbol{B} + t\boldsymbol{C}]]$$

$$= \frac{3t^2(1-t)}{V(t,\ \beta)^2}[\boldsymbol{D} - \boldsymbol{R}(t,\ 0,\ 0)],$$

where $V(t,\ \beta) = 3(1-t)^2 + 3t(1-t) + \beta t^2$. As β increases from 0 to ∞, for any fixed $t \in (0,\ 1)$, $\boldsymbol{R}(t,\ 0,\ \beta)$ moves along a straight line from point $\boldsymbol{R}(t,\ 0,\ 0)$ on edge ***BC*** towards ***D***. Moreover, for each fixed $\beta > 0$, $\boldsymbol{R}(t,\ 0,\ \beta)$, $t \in (0,\ 1)$, is a rational quadratic Bézier curve connecting ***B*** to ***D*** and hence it is planar and convex. Thus $\{\boldsymbol{R}(t,\ 0,\ \beta),\ t \in (0,\ 1):\ 0 < \beta < \infty\}$ is a nested family of planar curves, indexed by β, which fills the interior of triangle ***BCD***, as illustrated in Fig. 2.2.

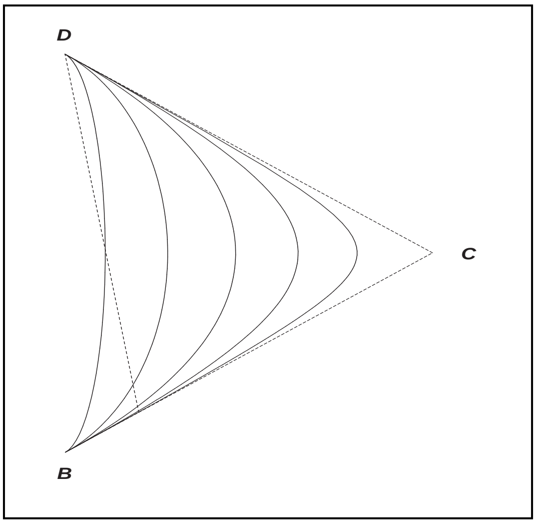

Fig. 2.2 Nested property of $\{\boldsymbol{R}(t,\ 0,\ \beta),\ t \in (0,\ 1):\ 0 < \beta < \infty\}$ and the locus line at $t = 0.2$.

With the above nested property of $\{\boldsymbol{R}(t,\ 0,\ \beta),\ t \in (0,\ 1):\ 0 < \beta < \infty\}$ and that a β-surface is made up of open line segments joining points of the rational quadratic curve $\boldsymbol{R}(t,\ 0,\ \beta)$, $t \in (0,\ 1)$ to ***A***, we obtain that the cone-shaped β-surfaces,

$0 < \beta < \infty$, form a nested family which fills the interior of tetrahedron ***ABCD***, see Fig. 2.3. Here the family of surfaces is nested where each surface of the family does not intersect any other surface in the family.

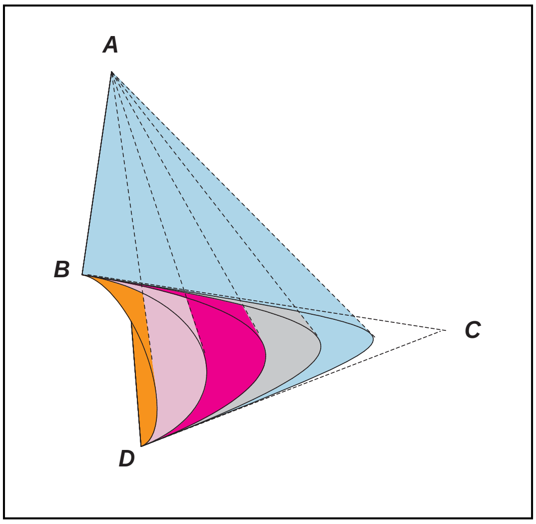

Fig. 2.3 Nested property of the β -surfaces.

2.1.2 α -Surface

A similar argument to that in subsection 2.1.1 leads to the formation of α -surfaces. As a consequence of (2.6), for any fixed $t_0 \in (0, 1)$ and $\alpha_0 > 0$, as β increases from 0 to ∞, $\boldsymbol{R}(t_0, \alpha_0, \beta)$ moves along a straight line from the point $\boldsymbol{R}(t_0, \alpha_0, 0)$ on the triangle ***ABC*** towards ***D***. This yields a cone-shaped constant α surface named the α_0 -surface, see Fig. 2.4(a). It consists of open line segments joining $\boldsymbol{R}(t, \alpha_0, 0)$ to ***D***, for every $t \in (0, 1)$. This surface also represents the family of nested curves indexed by β , $\{\boldsymbol{R}(t, \alpha_0, \beta), \ t \in (0, 1): \ 0 < \beta < \infty\}$, as illustrated in Fig. 2.4(b). For each fixed $\beta > 0$, the corresponding rational cubic curve connects ***A*** to ***D***.

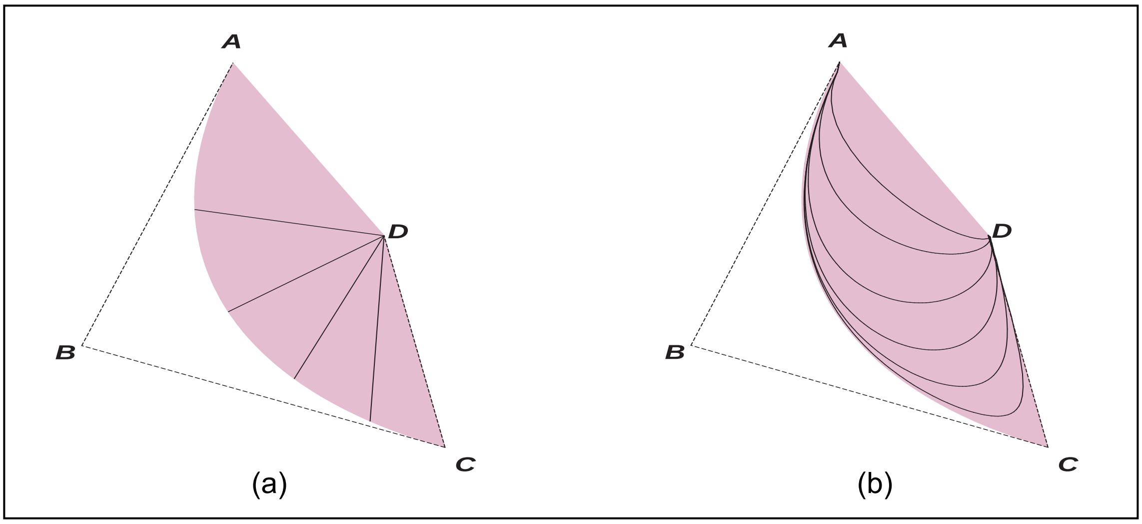

Fig. 2.4(a) α_0-surface, $\boldsymbol{R}(t,\ \alpha_0,\ \beta)$, $t \in (0,\ 1)$, $0 < \beta < \infty$, for a fixed $\alpha_0 > 0$, with some locus lines at $t = 0.2$, 0.4, 0.6, 0.8.

(b) Nested curves $\boldsymbol{R}(t,\ \alpha_0,\ \beta)$, $t \in (0,\ 1)$, for a fixed $\alpha_0 > 0$ and $\beta = 0.05$, 0.25, 1, 5, 50, 500, which lie on α_0-surface.

Similarly the set of rational quadratics $\{\boldsymbol{R}(t,\ \alpha,\ 0),\ t \in (0,\ 1):\ 0 < \alpha < \infty\}$, indexed by α, is a family of nested planar curves that fills the interior of the triangle ***ABC***, and the family of α-surfaces is nested and fills the interior of tetrahedron ***ABCD***.

Lastly we would like to note that the rational cubic curve $\boldsymbol{R}(t,\ \alpha,\ \beta)$, $t \in (0,\ 1)$ lies on the α-surface and β-surface. Hence it is the intersection of α-surface and β-surface, see Fig. 2.5.

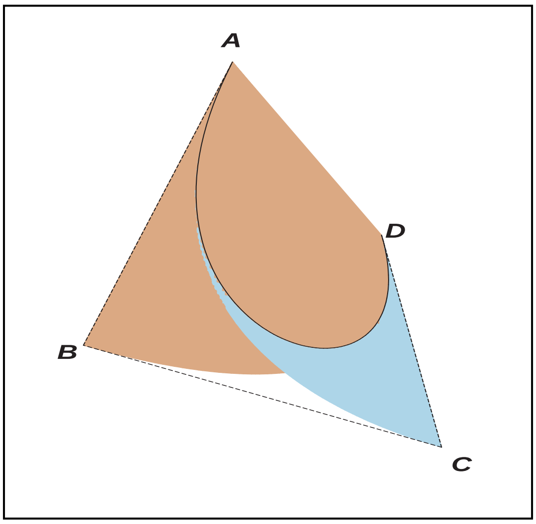

Fig. 2.5 Curve $\boldsymbol{R}(t,\ \alpha,\ \beta)$, $t \in (0,\ 1)$ is the intersection of the α-surface and β-surface.

2.2 *t*-Triangle

Next we would show another geometric structure named *t*-triangle. From (2.2), for any fixed $t_0 \in (0,\ 1)$, we can rewrite rational cubic Bézier as

$$\boldsymbol{R}(t_0,\ \alpha,\ \beta) = \frac{\alpha(1-t_0)^3}{W_0}\boldsymbol{A} + \frac{3t_0(1-t_0)}{W_0}[(1-t_0)\boldsymbol{B} + t_0\boldsymbol{C}] + \frac{\beta t_0^{\ 3}}{W_0}\boldsymbol{D}$$

$$= \frac{\alpha(1-t_0)^3}{W_0}\boldsymbol{A} + \frac{3t_0(1-t_0)}{W_0}\boldsymbol{R}(t_0,\ 0,\ 0) + \frac{\beta t_0^{\ 3}}{W_0}\boldsymbol{D},$$

where $W_0 = \alpha(1-t_0)^3 + 3t_0(1-t_0)^2 + 3t_0^{\ 2}(1-t_0) + \beta t_0^{\ 3}$. As each $\boldsymbol{R}(t_0,\ \alpha,\ \beta)$, $\alpha > 0$, $\beta > 0$, is a convex combination of three points $\boldsymbol{A}$, $\boldsymbol{S}_0 = \boldsymbol{R}(t_0,\ 0,\ 0)$ and $\boldsymbol{D}$, thus $\{\boldsymbol{R}(t_0,\ \alpha,\ \beta):\ 0 < \alpha < \infty,\ 0 < \beta < \infty\}$ is the interior of triangle $\boldsymbol{AS}_0\boldsymbol{D}$. We refer to the interior of the triangle $\boldsymbol{AS}_0\boldsymbol{D}$ as the t_0-triangle.

Observe that the limiting line segments $\boldsymbol{R}(t_0,\ 0,\ \beta)$ and $\boldsymbol{R}(t_0,\ \alpha,\ 0)$ obtained from $\boldsymbol{R}(t_0,\ \alpha,\ \beta)$ when $\alpha \to 0$ and $\beta \to 0$ respectively are

$$\boldsymbol{R}(t_0,\ 0,\ \beta) = \frac{3(1-t_0)}{V_0}\boldsymbol{S}_0 + \frac{\beta t_0^{\ 2}}{V_0}\boldsymbol{D}, \qquad \beta > 0,$$

and

$$\boldsymbol{R}(t_0,\ \alpha,\ 0) = \frac{\alpha(1-t_0)^2}{U_0}\boldsymbol{A} + \frac{3t_0}{U_0}\boldsymbol{S}_0, \qquad \alpha > 0,$$

where $V_0 = 3(1-t_0)^2 + 3t_0(1-t_0) + \beta t_0^{\ 2}$, $U_0 = \alpha(1-t_0)^2 + 3t_0(1-t_0) + 3t_0^{\ 2}$. These are the open line segments $\boldsymbol{S}_0\boldsymbol{D}$ and $\boldsymbol{S}_0\boldsymbol{A}$ respectively. The collection of all the layered *t*-triangles, $t \in (0,\ 1)$, fills the interior of the tetrahedron ***ABCD*** and each triangle does not intersect any other *t*-triangle (see Fig. 2.6).

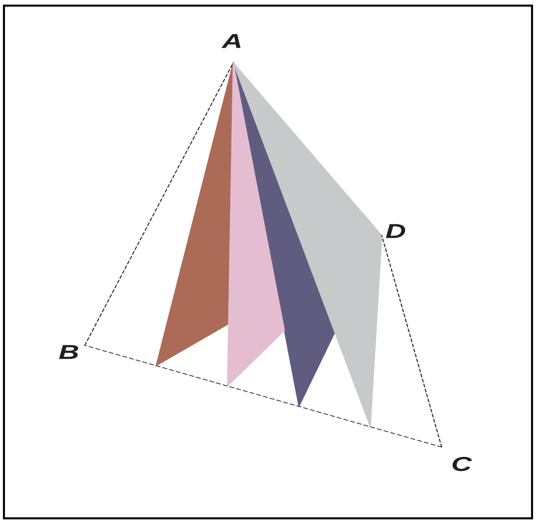

Fig. 2.6 Layered t-triangle, $t = 0.2,\ 0.4,\ 0.6,\ 0.8$.

2.3 Uniqueness of Representation

Based upon the discussions in previous sections, for the control points ***A***, ***B***, ***C***, ***D*** which are not coplanar, we have characterized $\{\boldsymbol{R}(t,\ \alpha,\ \beta):\ t \in (0,\ 1),\ 0 < \alpha < \infty,\ 0 < \beta < \infty\}$, as a 3D volume of the interior of the tetrahedron ***ABCD*** which can be "sliced" in any one of the following geometric structures:

(i) the set of nested α-surfaces, $0 < \alpha < \infty$,

(ii) the set of nested β-surfaces, $0 < \beta < \infty$,

(iii) the set of layered t-triangles, $t \in (0,\ 1)$.

Indeed every interior point of the tetrahedron ***ABCD*** has a unique representation of the form $\boldsymbol{R}(t,\ \alpha,\ \beta)$ as noted in Proposition 2.2.

Proposition 2.2

Given a point ***G*** in the interior of the tetrahedron ***ABCD*** where ***A***, ***B***, ***C*** and ***D*** are not coplanar, there exists a unique rational cubic curve $\boldsymbol{R}(t,\ \alpha,\ \beta)$, $t \in (0,\ 1)$, of the form (2.2) passing through it, i.e. there exists a unique $t_0 \in (0,\ 1)$, $\alpha_0 > 0$, $\beta_0 > 0$ such that $\boldsymbol{R}(t_0,\ \alpha_0,\ \beta_0) = \boldsymbol{G}$.

Proof:

We shall first find the t-triangle on which the point $\boldsymbol{G}$ lies. Let the point of projection of $\boldsymbol{A}$ onto the triangle $\boldsymbol{BCD}$ through point $\boldsymbol{G}$ be denoted as $\boldsymbol{Q}_1$, see Fig. 2.7. $\boldsymbol{AQ}_1$ is the line segment $\boldsymbol{R}(t_0, \alpha, \beta_0)$, $0 < \alpha < \infty$, for some $\beta_0 > 0$ and $t_0 \in (0, 1)$. Hence it can be interpreted as the intersection of the β_0-surface and the t_0-triangle. The point $\boldsymbol{D}$ is projected through $\boldsymbol{Q}_1$ to the edge $\boldsymbol{BC}$, with the point obtained be denoted as $\boldsymbol{S}_0$. The value t_0 can be evaluated easily from the linear equation $\boldsymbol{S}_0 = (1-t)\boldsymbol{B} + t\boldsymbol{C}$. β_0 can then be determined by the linear equation $\boldsymbol{Q}_1 = \boldsymbol{R}(t_0, 0, \beta)$ in β (see (3.1)). Lastly, since the line $\boldsymbol{AQ}_1$ passes through $\boldsymbol{G}$, then α_0 can be found from the linear equation $\boldsymbol{G} = \boldsymbol{R}(t_0, \alpha, \beta_0)$ in α (see (3.2)). Thus there exists t_0, α_0, β_0 such that $\boldsymbol{R}(t_0, \alpha_0, \beta_0) = \boldsymbol{G}$.

Alternatively we can find a solution $\boldsymbol{R}(t_1, \alpha_1, \beta_1) = \boldsymbol{G}$ by first projecting $\boldsymbol{D}$ through $\boldsymbol{G}$ to a point $\boldsymbol{Q}_2$ which lies on triangle $\boldsymbol{ABC}$, and then projecting $\boldsymbol{A}$ through $\boldsymbol{Q}_2$ to a point $\boldsymbol{S}_1$ on $\boldsymbol{BC}$. From this sequence of operations, the values of t_1, then α_1 and finally β_1 can be evaluated easily as above.

We now show that $(t_0, \alpha_0, \beta_0) = (t_1, \alpha_1, \beta_1)$. As we know the interior of the tetrahedron $\boldsymbol{ABCD}$ consists of layered t-triangles, $t \in (0, 1)$, which are the interior of triangles $\boldsymbol{ASD}$, where $\boldsymbol{S} = (1-t)\boldsymbol{B} + t\boldsymbol{C}$. Since these t-triangles do not intersect one another, so $\boldsymbol{G}$ lies on one and only one of the t-triangles, hence $t_0 = t_1$. Next we shall show that the two tuples (α_0, β_0) and (α_1, β_1) are identical. The first tuple is based on the β_0-surface and the projection point $\boldsymbol{Q}_1$, while the second tuple is based on the α_1-surface and the projection point $\boldsymbol{Q}_2$. Observe that $\boldsymbol{G}$ lies on the t_0-triangle which is the interior of the triangle $\boldsymbol{AS}_0\boldsymbol{D}$ with point $\boldsymbol{S}_0 = (1-t_0)\boldsymbol{B} + t_0\boldsymbol{C}$. $\boldsymbol{Q}_1$ and $\boldsymbol{Q}_2$ lie on open line segments $\boldsymbol{S}_0\boldsymbol{D}$ and $\boldsymbol{S}_0\boldsymbol{A}$ respectively. The line between the points $\boldsymbol{Q}_1$ and $\boldsymbol{A}$ is represented by $\boldsymbol{R}(t_0, \alpha, \beta_0)$, $0 < \alpha < \infty$, while the line between $\boldsymbol{Q}_2$ and $\boldsymbol{D}$ is

$\boldsymbol{R}(t_0,\ \alpha_1,\ \beta)$, $0 < \beta < \infty$. Since both lines pass through **G**, i.e. the point **G** is the intersection point of lines $\boldsymbol{R}(t_0,\ \alpha,\ \beta_0)$ and $\boldsymbol{R}(t_0,\ \alpha_1,\ \beta)$, hence $\alpha_0 = \alpha_1$ and $\beta_1 = \beta_0$.

For uniqueness, suppose that $\boldsymbol{R}(t,\ \alpha,\ \beta) = \boldsymbol{G}$. Then the value of t, α and β can be determined by either one of the two approaches described above and thus the solution set is unique. □

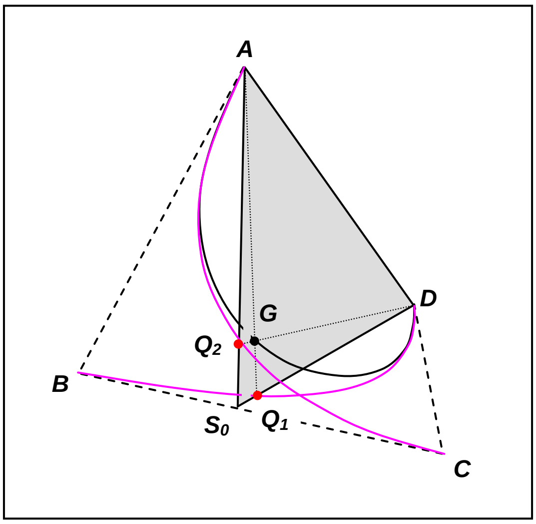

Fig. 2.7 Geometric view of the unique representation $\boldsymbol{R}(t,\ \alpha,\ \beta)$ for a space point **G**.

Observe that $\boldsymbol{G} = \boldsymbol{R}(t_0,\ \alpha_0,\ \beta_0)$ lies on the t_0-triangle. If **A**, **B**, **C**, **D** are coplanar, we obtain an infinite set of *t*-triangles that contained **G**, hence there are an infinite number of representation of **G** in terms of *t*, α and β, see Fig. 2.8. However, as described in (Meek et. al, 2003), if we fix either one of the weights α or β, or the ratio of these two weights, or the *t* value, then a unique representation can be achieved when the polyline ***ABCD*** is "C-shaped", but if the polyline ***ABCD*** is "S-shaped", then the representation need not be unique.

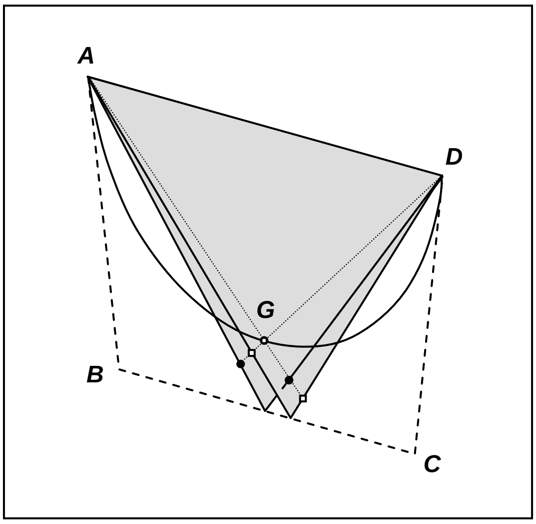

Fig. 2.8 Geometric view of two of the infinite representation $\boldsymbol{R}(t,\ \alpha,\ \beta)$ for a point $\boldsymbol{G}$ in the planar quadrilateral $\boldsymbol{ABCD}$.

2.4 $(\alpha,\ \beta)$-Surface

In this section we discuss the effect of scaling both weights α and β of $\boldsymbol{R}(t,\ \alpha,\ \beta)$ in (2.2) by a positive factor λ while keeping their ratio fixed. Consider

$$\boldsymbol{R}(t, \lambda\alpha, \lambda\beta) = \frac{\lambda\alpha(1-t)^3\boldsymbol{A} + 3t(1-t)^2\boldsymbol{B} + 3t^2(1-t)\boldsymbol{C} + \lambda\beta t^3\boldsymbol{D}}{\lambda\alpha(1-t)^3 + 3t(1-t)^2 + 3t^2(1-t) + \lambda\beta t^3}, \quad 0 \le t \le 1, \qquad (2.7)$$

where α, $\beta > 0$ are fixed and $\lambda > 0$. Observe that for $t \in (0,\ 1)$,

$$\lim_{\lambda\to 0}\boldsymbol{R}(t, \lambda\ \alpha,\ \lambda\beta) = (1-t)\boldsymbol{B} + t\boldsymbol{C}$$

and

$$\lim_{\lambda\to\infty}\boldsymbol{R}(t,\ \lambda\alpha,\ \lambda\beta) = \frac{\alpha(1-t)^3}{\alpha(1-t)^3 + \beta t^3}\boldsymbol{A} + \frac{\beta t^3}{\alpha(1-t)^3 + \beta t^3}\boldsymbol{D},$$

and these limits are denoted as $\boldsymbol{R}(t,\ 0,\ 0)$ and $\boldsymbol{R}(t,\ \infty,\ \infty)$ respectively.

The first partial derivative of $\boldsymbol{R}(t,\ \lambda\alpha,\ \lambda\beta)$ with respect to λ is

$$\frac{\partial\boldsymbol{R}}{\partial\lambda}(t,\ \lambda\alpha,\ \lambda\beta) = \frac{3t(1-t)[\alpha(1-t)^3 + \beta t^3]}{\eta(t,\ \lambda,\ \alpha,\ \beta)^2}\left[\frac{\alpha(1-t)^3\boldsymbol{A} + \beta t^3\boldsymbol{D}}{\alpha(1-t)^3 + \beta t^3} - [(1-t)\boldsymbol{B} + t\boldsymbol{C}]\right]$$

$$= \frac{3t(1-t)[\alpha(1-t)^3 + \beta t^3]}{\eta(t, \lambda, \alpha, \beta)^2}[\boldsymbol{R}(t, \infty, \infty) - \boldsymbol{R}(t, 0, 0)],$$

where $\eta(t, \lambda, \alpha, \beta) = \lambda\alpha(1-t)^3 + 3t(1-t)^2 + 3t^2(1-t) + \lambda\beta t^3$. Hence for any fixed $t \in (0, 1)$, as λ increases from 0 to ∞, $\boldsymbol{R}(t, \lambda\alpha, \lambda\beta)$ moves along a straight line from $\boldsymbol{R}(t, 0, 0)$ towards $\boldsymbol{R}(t, \infty, \infty)$. The set of open line segments indexed by $t \in (0, 1)$, joining $\boldsymbol{R}(t, 0, 0)$ to $\boldsymbol{R}(t, \infty, \infty)$, form a surface which is referred to as an (α, β)-surface as illustrated in Fig. 2.9(a). This (α, β)-surface also represents the family of curves $\{\boldsymbol{R}(t, \lambda\alpha, \lambda\beta),\ t \in (0, 1):\ 0 < \lambda < \infty\}$, indexed by λ, as shown in Fig. 2.9(b). When λ decreases, $\boldsymbol{R}(t, \lambda\alpha, \lambda\beta)$, $t \in (0, 1)$, approaches the line segment ***BC*** while λ increases, it will approach the line segment ***AD***. Thus the family of curves $\{\boldsymbol{R}(t, \lambda\alpha, \lambda\beta),\ t \in (0, 1):\ 0 < \lambda < \infty\}$ is nested.

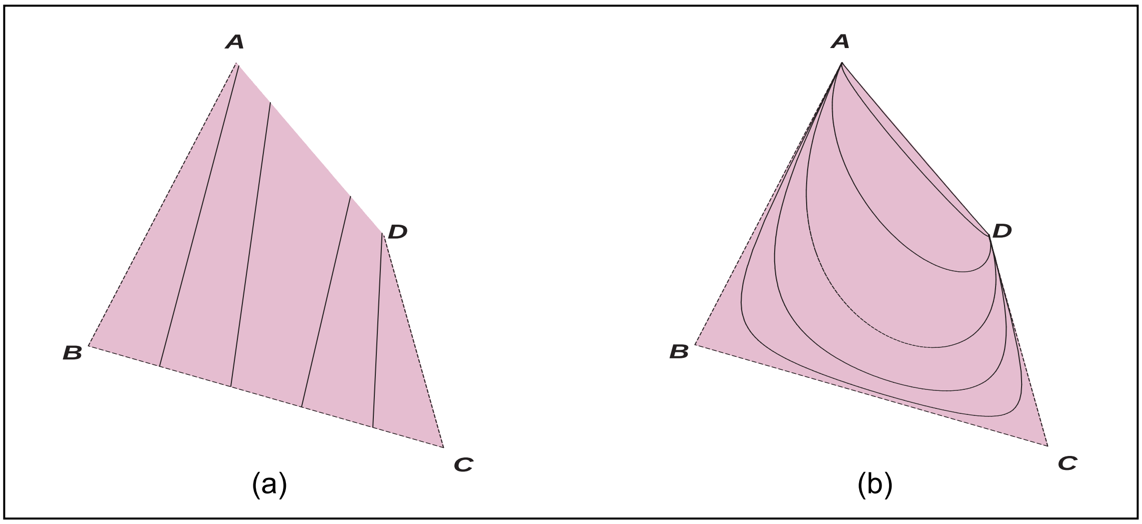

Fig. 2.9(a) (α, β)-surface, $\boldsymbol{R}(t, \lambda\alpha, \lambda\beta)$, $t \in (0, 1)$, $0 < \lambda < \infty$, for fixed α, $\beta > 0$, with some locus lines at $t = 0.2, 0.4, 0.6, 0.8$.

(b) Nested curves $\boldsymbol{R}(t, \lambda\alpha, \lambda\beta)$, $t \in (0, 1)$, $\lambda = 0.05, 0.25, 1, 5, 50, 500$, which lie on (α, β)-surface.

CHAPTER 3
THE POINT OF CONTACT BETWEEN THE RATIONAL CUBIC CURVE AND A PLANE

In the previous chapter, we have described that for any point $\boldsymbol{G}$ in the interior of the tetrahedron ***ABCD***, there exists a unique $(t,\ \alpha,\ \beta)$ of the curve (2.2) such that $\boldsymbol{R}(t,\ \alpha,\ \beta)=\boldsymbol{G}$. To attain this, first we project $\boldsymbol{A}$ through $\boldsymbol{G}$ to a point $\boldsymbol{Q}_1=\boldsymbol{R}(t,\ 0,\ \beta)$ which lies on the triangle ***BCD*** (see Fig. 2.7) and then project $\boldsymbol{D}$ through $\boldsymbol{Q}_1$ to a point $\boldsymbol{S}=\boldsymbol{R}(t,\ 0,\ 0)$ that lies on the edge ***BC***. Thus the value of t can be found easily from the linear equations of

$$\boldsymbol{S}=(1-t)\boldsymbol{B}+t\boldsymbol{C}.$$

The value of β can then be computed from the linear equation $\boldsymbol{Q}_1=\boldsymbol{R}(t,\ 0,\ \beta)$ in β

$$[3(1-t)^2+3t(1-t)+\beta t^2]\boldsymbol{Q}_1=3(1-t)\boldsymbol{S}+\beta t^2\boldsymbol{D}$$

that gives

$$\beta t^2(\boldsymbol{Q}_1-\boldsymbol{D})=3(1-t)(\boldsymbol{S}-\boldsymbol{Q}_1). \tag{3.1}$$

Finally the value of α can be determined from the linear equation $\boldsymbol{G}=\boldsymbol{R}(t,\ \alpha,\ \beta)$ in α

$$[\alpha(1-t)^3+3t(1-t)^2+3t^2(1-t)+\beta t^3]\boldsymbol{G}=\alpha(1-t)^3\boldsymbol{A}+3t(1-t)\boldsymbol{S}+\beta t^3\boldsymbol{D}$$

that yields

$$\alpha(1-t)^3(\boldsymbol{G}-\boldsymbol{A})=3t(1-t)(\boldsymbol{S}-\boldsymbol{G})+\beta t^3(\boldsymbol{D}-\boldsymbol{G}). \tag{3.2}$$

Suppose that a point $\boldsymbol{H}$ on the $(\alpha,\ \beta)$-surface is given. A unique tuple $(t,\ \lambda)$ of the curve (2.7) from the family $\{\boldsymbol{R}(t,\ \lambda\alpha,\ \lambda\beta),\ t\in(0,\ 1):\ 0<\lambda<\infty\}$ which passes through $\boldsymbol{H}$ can be found. We can determine the tuple $(t,\ \lambda)$ by first finding the value t where the line segment through the points $\boldsymbol{R}(t,\ 0,\ 0)$ and $\boldsymbol{R}(t,\ \infty,\ \infty)$ passes through $\boldsymbol{H}$. Thus we have

$$[\boldsymbol{H}-\boldsymbol{R}(t,\ 0,\ 0)]\times[\boldsymbol{R}(t,\ \infty,\ \infty)-\boldsymbol{R}(t,\ 0,\ 0)]=\boldsymbol{0},$$

a quartic equation in t

$$\alpha(1-t)^4(\boldsymbol{A}-\boldsymbol{H})\times(\boldsymbol{B}-\boldsymbol{H})+\alpha t(1-t)^3(\boldsymbol{A}-\boldsymbol{H})\times(\boldsymbol{C}-\boldsymbol{H})+ \\ \beta t^3(1-t)(\boldsymbol{D}-\boldsymbol{H})\times(\boldsymbol{B}-\boldsymbol{H})+\beta t^4(\boldsymbol{D}-\boldsymbol{H})\times(\boldsymbol{C}-\boldsymbol{H}) \quad = \quad \boldsymbol{0},$$

where "$\times$" stands for the cross product and $\boldsymbol{0}$ denotes a zero vector. Since the family of curves $\{\boldsymbol{R}(t,\ \lambda\alpha,\ \lambda\beta\},\ t\in(0,\ 1):\ 0<\lambda<\infty\}$ is nested, there is exactly one root $t\in(0,\ 1)$ for this quartic equation which can be found numerically. The value of λ can then be evaluated from the linear equation $\boldsymbol{H}=\boldsymbol{R}(t,\ \lambda\alpha,\ \lambda\beta)$ in λ

$$[\lambda\alpha(1-t)^3+3t(1-t)^2+3t^2(1-t)+\lambda\beta t^3]\boldsymbol{H} \\ = \quad \lambda\alpha(1-t)^3\boldsymbol{A}+3t(1-t)^2\boldsymbol{B}+3t^2(1-t)\boldsymbol{C}+\lambda\beta t^3\boldsymbol{D}$$

that gives

$$\lambda[\alpha(1-t)^3(\boldsymbol{H}-\boldsymbol{A})+\beta t^3(\boldsymbol{H}-\boldsymbol{D})]=3t(1-t)(\boldsymbol{S}-\boldsymbol{H}).$$

Next we shall describe the necessary and sufficient conditions for a rational cubic to touch a given plane. In (Goodman et al., 1991) interpolation to planar data points that lie on one side of one or more lines has been considered. Conditions are given for a parametric rational cubic curve not to cross a given line when the two end points of the curve lie strictly on one side of the line. Meek et al. (2003) extended this result to allow a polyline as a more general constraint where all the data points need not lie on one side of the infinite line through each of its edges. An interpolating curve is constructed to a given set of planar data points where both the data points and the interpolating curve lie on the same side of the polyline. Let us recall the following result quoted from (Meek et al., 2003) on the zeros of multiplicities 2 or 3 of a cubic Bernstein polynomial in $(0,\ 1)$.

Lemma 3.1

Let $g(t)=a(1-t)^3+3bt(1-t)^2+3ct^2(1-t)+dt^3$, $t\in[0,\ 1]$, where $a,\ b,\ c,\ d\in\nabla$.

(i) $g(t)$ has a zero of multiplicity 2 in $(0,\ 1)$ if and only if

$$(ad-bc)^2 = 4(ac-b^2)(bd-c^2)$$

and

$$(ad-bc)(ac-b^2) < 0 \qquad \text{[equivalently } (ad-bc)(bd-c^2) < 0\text{]}.$$

This zero occurs at $\xi \in (0,\ 1)$ where

$$\frac{\xi}{\xi-1} = \frac{2(ac-b^2)}{ad-bc} = \frac{ad-bc}{2(bd-c^2)} < 0\,.$$

(ii) $g(t)$ has a zero of multiplicity 3 in $(0,\ 1)$ if and only if

$$\frac{a}{b} = \frac{b}{c} = \frac{c}{d} < 0\,.$$

This zero occurs at $\xi \in (0,\ 1)$ where

$$\frac{\xi}{\xi-1} = \frac{a}{b} = \frac{b}{c} = \frac{c}{d} < 0\,.$$

Consider the parametric rational cubic Bézier $\boldsymbol{R}(t,\ \alpha,\ \beta)$, $t \in [0,\ 1]$, given in (2.2) where α, $\beta > 0$ are fixed. $\boldsymbol{R}(t,\ \alpha,\ \beta)$ touches the plane $z = 0$ at $t = t_0 \in (0,\ 1)$ if for normal vector $\boldsymbol{n} = (0,\ 0,\ 1)^T$,

$$\boldsymbol{n} \bullet \boldsymbol{R}(t_0,\ \alpha,\ \beta) = 0\,,$$

and there exist $\varepsilon > 0$ such that

$$\boldsymbol{n} \bullet \boldsymbol{R}(t,\ \alpha,\ \beta) > 0\,, \qquad \forall\, t \in (t_0-\varepsilon,\ t_0+\varepsilon) \setminus \{t_0\}$$

or

$$\boldsymbol{n} \bullet \boldsymbol{R}(t,\ \alpha,\ \beta) < 0\,, \qquad \forall\, t \in (t_0-\varepsilon,\ t_0+\varepsilon) \setminus \{t_0\}\,,$$

where "$\bullet$" denotes the dot product. These two statements are equivalent to the rational cubic function $h(t) = \boldsymbol{n} \bullet \boldsymbol{R}(t,\ \alpha,\ \beta)$, $t \in [0,\ 1]$, having a zero of multiplicity 2 or 3 at $t = t_0$. We note that a smooth rational function with non-vanishing denominator has a multiple zero if and only if its numerator has a zero of the same multiplicity at the same point. Moreover, the Bézier representation is affine invariant and via rotation and translation which are affine transformations, any given constraint plane $a_0 x + a_1 y + a_2 z + a_3 = 0$, $a_j \in \nabla$, $0 \le j \le 4$, may be transformed to the plane $z = 0$. With these observations, we derive directly from Lemma 3.1 the necessary and sufficient conditions for the rational cubic $\boldsymbol{R}(t,\ \alpha,\ \beta)$, $t \in [0,\ 1]$ to touch a given plane as given in Proposition 3.1.

Proposition 3.1

Consider the parametric rational cubic Bézier curve $\boldsymbol{R}(t,\ \alpha,\ \beta)$, $t \in [0,\ 1]$, of (2.2) where α, $\beta > 0$ and a given constraint plane. Let *a*, *b*, *c*, *d* be respectively the signed distances of the control points ***A***, ***B***, ***C***, ***D*** of $\boldsymbol{R}(t,\ \alpha,\ \beta)$ from the constraints plane, with points on one side of the constraint plane having positive distances while points on the other side having negative distances. Then $\boldsymbol{R}(t,\ \alpha,\ \beta)$ is tangent to the constraint plane at $\xi \in (0,\ 1)$ if and only if one of the following two conditions holds

(i) $(\alpha\beta ad - bc)^2 = 4(\alpha ac - b^2)(\beta bd - c^2)$

and

$(\alpha\beta ad - bc)(\alpha ac - b^2) < 0$ [equivalently $(\alpha\beta ad - bc)(\beta bd - c^2) < 0$],

(ii) $\dfrac{\alpha a}{b} = \dfrac{b}{c} = \dfrac{c}{\beta d} < 0$.

With condition (i), a zero of multiplicity 2 occurs at $\xi \in (0,\ 1)$ where

$$\frac{\xi}{\xi - 1} = \frac{2(\alpha ac - b^2)}{\alpha\beta ad - bc} = \frac{\alpha\beta ad - bc}{2(\beta bd - c^2)} < 0,$$

while with condition (ii) a zero of multiplicity 3 occurs at $\xi \in (0,\ 1)$ where

$$\frac{\xi}{\xi - 1} = \frac{\alpha a}{b} = \frac{b}{c} = \frac{c}{\beta d} < 0.$$